Radiative association of LiH($X\ ^1\Sigma^+$) from electronically excited lithium atoms

F. A. Gianturco* and P. Gori Giorgi
Department of Chemistry, The University of Rome, Città Universitaria, 00185 Rome, Italy
(Received 18 June 1996)

Full quantum calculations are carried out for the collisional processes involving H atoms in their ground electronic state and electronically excited lithium atoms, Li($1s^2 2p$). The channels that are being considered are those leading to the formation of bound rotovibrational states of LiH($X\ ^1\Sigma^+$). The effects of both the specific features of the involved electronic potential-energy curves and of the transition moments coupling bound and continuum states during the process are studied in relation to the low-energy behavior of the corresponding cross sections. The role of the multitude of open channel resonances on the final rate constants is also analyzed and discussed over a broad range of bath temperatures. [S1050-2947(96)05011-1]

PACS number(s): 33.80.Gj, 33.90.+h, 34.50.Bw

I. INTRODUCTION

The LiH molecule has been widely studied in the last few years because of the possible importance of its role in observational cosmology [1–7]. In the framework of the hot big bang model (see, for example [8]), in fact, the first stellar objects are supposed to be formed in a gas consisting of H, ^{2}H, ^{3}He, ^{4}He, and ^{7}Li and hence, before a first generation of stars, LiH and LiH^+ are the only available molecular species that, given their high permanent dipole moment, can interact with cosmic background radiation (CBR) photons.

It has been shown [2,3] that the presence of the LiH molecule in the early universe, if its abundance were not too low, could have produced a partial smearing of primary CBR anisotropies and could be used to detect primordial clouds.

Stancil *et al.* [5] have recently developed a model of the kinetics of the lithium chemistry in the early universe, and the primordial LiH abundance is found to be much lower than the one needed to produce relevant observational effects. Such a low LiH abundance is primarily due to the small value of the rate constants for the main LiH formation mechanism in the early universe environment, i.e., the direct radiative association [4,7]

$$\mathrm{Li}(1s^2 2s)+\mathrm{H}(1s)\rightarrow \mathrm{LiH}(X\ ^1\Sigma^+)+h\nu. \qquad (1)$$

This process implies a free-bound transition between states belonging to the same adiabatic potential-energy curve, and therefore its probability of occurring is not very large [4,7].

The results of Stancil *et al.* seem to exclude any smearing of CBR anisotropies by LiH molecules and any possibility of observing primordial clouds in which the density would be too low to activate alternative molecular formation mechanisms. Maiani *et al.* [9] have recently investigated the possibility of detecting LiH molecules in giant molecular clouds in galaxies, in which the chemistry should be rather different from that acting in the early universe. Maiani *et al.* [9] therefore suggested that the detection of LiH in our galaxy could have a great impact in the final estimate of Li abundance.

In order to further investigate the implications of such a different environment one should be able to also evaluate the radiative recombination rates of initial atoms in different electronic states. To this end, we decided to carry out a fully quantum-mechanical treatment of the following process:

$$\mathrm{Li}(1s^2 2p)+\mathrm{H}(1s)\rightarrow \mathrm{LiH}(X\ ^1\Sigma^+)+h\nu. \qquad (2)$$

Process (2) can, in fact, be relevant for the LiH molecule formation in our galaxy, given the presence of an optical wavelength background radiation that can produce excited lithium atoms in different electronic configurations.

It is also worth noting at this point that process (2) is much more efficient than process (1) because it implies free-bound transitions between states belonging to different potential-energy curves, and therefore spontaneous emission has a greater probability of occurring. It would not have been available in the early universe because of the low radiation temperature at the relevant epochs.

II. THEORY

Direct two-body association only becomes possible if the residual energy is released radiatively through photon emission. A fully quantum-mechanical photoassociation theory can be formulated and used to calculate the cross section at various collision energies E from which one obtains, in turn, the rate coefficient at various bath temperatures T [10,11,7].

Within the range of validity of the Born-Oppenheimer (BO) approximation, the wave function of the two colliding partners can be written as a superposition of partial waves that are the solutions of the Schrödinger radial equation with a potential $V(R)$ corresponding to one particular BO potential-energy curve. The cross section is given, in atomic units, by [10,7]

$$\sigma(E)=\frac{64}{3}\frac{\pi^5}{c^3}\frac{p}{k^2}\sum_{v'J'J}\nu^3_{E,v',J'}S_{JJ'}M^2_{v'J',EJ}, \qquad (3)$$

*Mailing address: Professor F. A. Gianturco, Dipartimento di Chimica, Città Universitaria, 00185 Rome, Italy. Fax: +39-6-49913305. Electronic address: FAGIANT@CASPUR.IT

where $k^2=2\mu E$, p is the statistical weight of the initial potential-energy curve (PEC), ν is the emitted photon frequency, $S_{JJ'}$ is the Hönl-London coefficient, and

$$M_{v'J',EJ}=\int_0^\infty \phi_{v'J'}(R)\mu(R)f_{EJ}(R)dR \tag{4}$$

is the matrix element of the transition moment $\mu(R)$ between the final bound state $|v'J'\rangle$ (normalized to unity) and the initial energy-normalized partial wave $|EJ\rangle$.

Since we are dealing with radiative processes, the allowed J and J' values are related by dipole selection rules, i.e., $J'=J\pm1$ for $\Sigma\rightarrow\Sigma$ transitions, and $J'=J$, $J\pm1$ for $\Lambda\rightarrow\Lambda'$ transitions with Λ and/or $\Lambda'\neq0$. Hence the number of partial waves is given, for each final vibrational state v', by $J_{\max}(v')+1$, where $J_{\max}(v')$ is the highest rotational level for the vibrational state v'.

The BO potential-energy curves that correspond asymptotically to the Li$(1s^22p)$+H$(1s)$ atomic partners are given by $A\ ^1\Sigma^+$, $B\ ^1\Pi$, $c\ ^3\Sigma^+$, and $b\ ^3\Pi$. Of them, the only two PEC's that can combine radiatively with the LiH ground state ($X\ ^1\Sigma^+$) are the $A\ ^1\Sigma^+$ and the $B\ ^1\Pi$ ones. The statistical weights are 1/12 for the former and 1/6 for the latter. The Hönl-London coefficients are given by [12]

$$\begin{aligned} J'=J+1\rightarrow S_{JJ'}=J+1,\\ J'=J-1\rightarrow S_{JJ'}=J \end{aligned} \tag{5}$$

for the $A\ ^1\Sigma^+\rightarrow X\ ^1\Sigma^+$ transition, and by [12]

$$\begin{aligned} J'=J+1\rightarrow S_{JJ'}=\frac{J}{4},\\ J'=J\rightarrow S_{JJ'}=\frac{2J+1}{4},\\ J'=J-1\rightarrow S_{JJ'}=\frac{J+1}{4} \end{aligned} \tag{6}$$

for the $B\ ^1\Pi\rightarrow X\ ^1\Sigma^+$ transition. Considering the distribution over final vibrational bound states that are formed in the recombination process, one notes that the total cross section can be written as

$$\sigma(E)=\sum_{v=0}^{v_{\max}}\sigma_v(E), \tag{7}$$

where $\sigma_v(E)$ is the partial cross section for the channel corresponding to the final vibrational state v, and is given by [7]

$$\sigma_v(E)=\frac{64}{3}\frac{\pi^5}{c^3}\frac{p}{k^2}\sum_{J=0}^{J_{\max}}\{\nu_{E,vJ}^3[JM_{vJ,EJ-1}^2+(J+1)M_{vJ,EJ+1}^2]\} \tag{8}$$

for the $A\ ^1\Sigma^+\rightarrow X\ ^1\Sigma^+$ transition, and by

$$\sigma_v(E)=\frac{16}{3}\frac{\pi^5}{c^3}\frac{p}{k^2}\left(\sum_{J=1}^{J_{\max}}\{\nu_{E,vJ}^3[(J-1)M_{vJ,EJ-1}^2+(2J+1)M_{vJ,EJ}^2+(J+2)M_{vJ,EJ+1}^2]\}+2\nu_{E,v0}^3M_{v0,E1}^2\right) \tag{9}$$

for the $B\ ^1\Pi\rightarrow X\ ^1\Sigma^+$ transition. The notation $J_{\max}$ means $J_{\max}(v)$, and in our calculations we have grouped together terms corresponding to the same value of the emitted photon frequency. As we have noted elsewhere [7], Eq. (8) is slightly different from the one given in Ref. [11] because of this specific choice in our analysis. In our case all possible final values of J are being considered in counting the contributions to Eqs. (8) and (9) with the correct frequency weighting. To further obtain the corresponding rates requires an additional integration over the Maxwellian distribution of the partner's relative velocities at a given temperature T, i.e., in atomic units one can write

$$K(T)=\left(\frac{8}{\mu\pi}\right)^{1/2}\left(\frac{1}{k_BT}\right)^{3/2}\int_0^\infty E\sigma(E)e^{-E/k_BT}dE. \tag{10}$$

III. DETAILS OF COMPUTATIONS

A. The molecular data

The $B\ ^1\Pi$ adiabatic PEC employed in the present work has been computed earlier by Boutalib and Gadea [13], who employed a nonempirical pseudopotential model for Li and a full configuration-interaction (CI) treatment of the valence electrons. Core-valence correlation effects were taken into account following a core-polarization potential method according to the formulation of Foucrault *et al.* [14] that reproduced very well the atomic lithium spectral properties.

The two Σ^+ PEC's involved, i.e., the $X\ ^1\Sigma^+$ and the $A\ ^1\Sigma^+$ ones, together with the transition moment between them have been computed by Berriche [15], who used the pseudopotential approach of Boutalib and Gadea [13]. He employed a denser set of points to evaluate the full potential-energy curves and introduced a further correction due to the variation of the electron affinity of the $X\ ^1\Sigma^+$ state as a function of the internuclear distance for the H atom. A detailed description of Berriche's $X\ ^1\Sigma^+$ adiabatic PEC can be found in Ref. [6].

Finally, the transition moment $B\ ^1\Pi\rightarrow X\ ^1\Sigma^+$ has been taken from Partridge and Langhoff [16], who carried out extensive CI calculations using a $22\sigma12\pi7\delta$ Slater-type orbital (STO) basis set to describe the molecular target electronic states.

The adiabatic PEC's and transition moments that we have used are reported in Fig. 1. One clearly sees there that the two electronically excited PEC's are very different in shape and can support a very different number of bound states: in either state such levels are much fewer than those that exist for the electronic ground state [6], a feature that will also affect the present findings, as we shall report below. Furthermore, the behavior of the two transition dipole moments is also very different: the Σ-Σ transition has a clear maximum at intermediate relative distances, while the Π-Σ transition

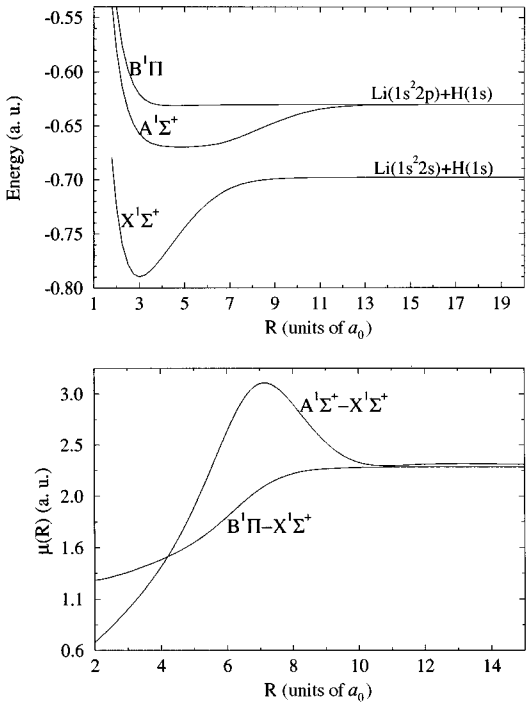

FIG. 1. Potential-energy curves and transition moments for the processes considered in this work. Top diagrams: $X\ ^1\Sigma^+$ curve from Ref. [6]; $A\ ^1\Sigma^+$ curve from Ref. [15]; $B\ ^1\Pi$ curve from Ref. [13]. Bottom diagram: Σ-Σ transition moment from Ref. [15]; Π-Σ transition moment from Ref. [16].

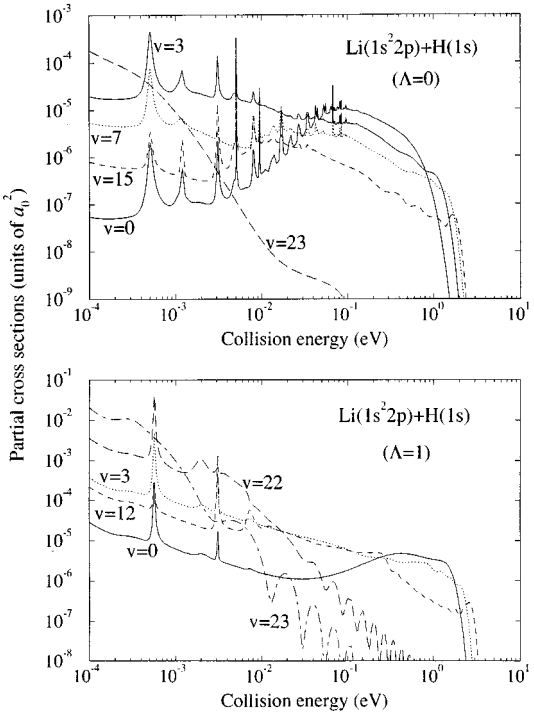

FIG. 2. Partial cross sections for the $\Lambda=0$ (upper part) and for the $\Lambda=1$ (lower part) processes. In both sets of curves the reported vibrational level refers to the final bound state of the $X\ ^1\Sigma^+$ molecular curve.

simply goes through a largely flat region of slightly increasing values. The bearings of such differences on the final cross sections will also be discussed in Sec. III B.

B. The computed cross sections

Starting from Eqs. (8) and (9), the corresponding partial cross sections have been computed for 451 collision energy values between 10^{-4} and 10 eV. Radial wave functions for both bound and continuum states have been generated using the Numerov method (see, for example, [17]) and the numerical stability of the results has been tested with the use of various point grids during propagation.

In Fig. 2 we have reported some of the partial cross sections for the two processes $A\ ^1\Sigma^+ \rightarrow X\ ^1\Sigma^+$ and $B\ ^1\Pi \rightarrow X\ ^1\Sigma^+$. The $X\ ^1\Sigma^+$ state has 24 ($v_{\max}=23$) vibrational levels; the ground state $v=0$ evidently is not the most probable final state for the radiative recombination event. Radiative association processes seem, therefore, to produce most probably vibrationally excited bound molecules, as we also found in our previous work [7]. This is due primarily to Frank-Condon factors, which are larger for the highest vibrational levels of the final molecule, and to the peculiar behavior of the transition moments discussed in Sec. III A. In any event, both processes appear to occur with fairly large partial cross sections and with fractional probabilities that, in the case with $\Lambda=0$, cover quite a broad range of values at low collision energies. We think that this is once more the manifestation of the pronounced maximum in the transition moment shown by Fig. 1.

One also notes that shape resonances are much more present in the process $A\ ^1\Sigma^+ \rightarrow X\ ^1\Sigma^+$ than in the

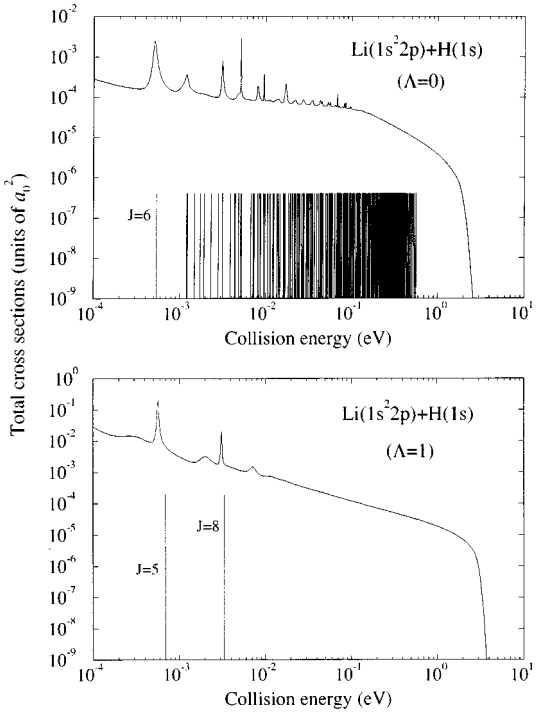

FIG. 3. Total cross sections for the $\Lambda=0$ (upper part) and for the $\Lambda=1$ (lower part) processes. In both diagrams some of the J values reported refer to the dominant contribution to the resonances shown above.

TABLE I. Computed rate coefficients for the $\Lambda=0$ and $\Lambda=1$ processes.

	$K(T)$ ($\mathrm{cm^3\,s^{-1}}$)	
T (K)	$A\ ^1\Sigma^+ \rightarrow X\ ^1\Sigma^+$	$B\ ^1\Pi \rightarrow X\ ^1\Sigma^+$
5	2.72×10^{-16}	1.10×10^{-14}
10	2.94×10^{-16}	8.93×10^{-15}
20	3.47×10^{-16}	6.98×10^{-15}
30	3.83×10^{-16}	6.02×10^{-15}
50	4.14×10^{-16}	4.97×10^{-15}
80	4.36×10^{-16}	4.16×10^{-15}
100	4.47×10^{-16}	3.82×10^{-15}
150	4.73×10^{-16}	3.29×10^{-15}
200	4.96×10^{-16}	2.96×10^{-15}
300	5.32×10^{-16}	2.56×10^{-15}
400	5.57×10^{-16}	2.32×10^{-15}
500	5.72×10^{-16}	2.16×10^{-15}
600	5.80×10^{-16}	2.04×10^{-15}
700	5.83×10^{-16}	1.94×10^{-15}
800	5.83×10^{-16}	1.86×10^{-15}
900	5.80×10^{-16}	1.80×10^{-15}
1000	5.75×10^{-16}	1.74×10^{-15}
1200	5.62×10^{-16}	1.65×10^{-15}
1500	5.39×10^{-16}	1.54×10^{-15}
2000	4.99×10^{-16}	1.42×10^{-15}
2500	4.62×10^{-16}	1.33×10^{-15}
3000	4.3×10^{-16}	1.3×10^{-15}
3500	4.0×10^{-16}	1.2×10^{-15}
4000	3.7×10^{-16}	1.1×10^{-15}
4500	3.5×10^{-16}	1.1×10^{-15}
5000	3.3×10^{-16}	1.1×10^{-15}
6000	2.9×10^{-16}	9.9×10^{-16}
7000	2.6×10^{-16}	9.2×10^{-16}

$B\ ^1\Pi \rightarrow X\ ^1\Sigma^+$ one: the $B\ ^1\Pi$ state is much less bound than the $A\ ^1\Sigma^+$ one, so it has only two pseudobound states, the energies and J values of which are reported in the lower part of Fig. 3, together with the total cross section for the $\Lambda=1$ process. The pseudobound states of the $A\ ^1\Sigma^+$ PEC, on the other hand, are much more numerous, as is also shown in the upper part of Fig. 3, and it is not possible to label each of them with its J value because of the marked spectral congestion exhibited as the collision energy increases. Energy and J values of pseudobound states have been computed using the method described by Le Roy and co-workers [18,19] and allow us to locate the open-channel resonances quite precisely.

The results shown in Fig. 3 also confirm what was mentioned before, i.e., that the final total cross sections are generally greater for the $\Lambda=1$ process than for the $\Lambda=0$ one. This is due to the features of the two electronically excited PEC's: the $A\ ^1\Sigma^+$ PEC is strongly bound, so Franck-Condon factors should be greater for transitions involving initial and final bound states rather than initial continuum and final bound states, especially for a system like the present one where the A and X minimum energy radial positions are not greatly displaced with respect to each other. On the other hand, the $B\ ^1\Pi$ PEC is weakly bound, so in this case Franck-Condon factors are greater for the free-bound transitions than for the bound-bound ones. Moreover, the $B\ ^1\Pi \rightarrow X\ ^1\Sigma^+$ transition is favored by dipole selection rules, which allow also transitions with $\Delta J=0$. Furthermore, the different features of the two transition moments also indicate that the one associated with the Π-Σ transition extends over a broad range of distances and therefore can efficiently couple several continuum states with the localized final bound states.

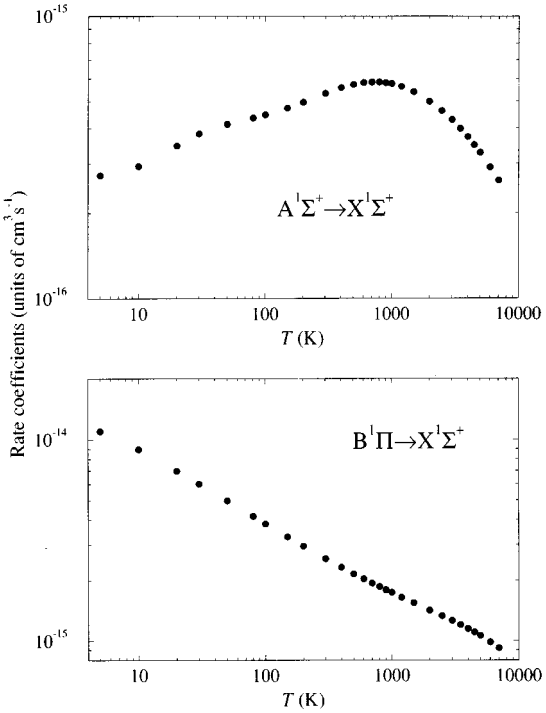

FIG. 4. Rate coefficients for the $\Lambda=0$ (upper part) and for the $\Lambda=1$ (lower part) processes. Both quantities are reported in a log-log scale as a function of temperature.

C. The computed rate coefficients

Rate coefficients for the two processes have been computed by numerical quadrature of Eq. (10) for a set of temperatures ranging from 5 to 7000 K. They are reported in Table I and shown in Fig. 4.

Rate coefficients for the $\Lambda=1$ process turned out to be in good agreement with a power-law behavior

$$K_{\Lambda=1}(T)=1.86\times10^{-14}\ T^{-0.34}\ \mathrm{cm^3\,s^{-1}}, \qquad (11)$$

while the $A\ ^1\Sigma^+ \rightarrow X\ ^1\Sigma^+$ process shows rather different features in its temperature dependence. In particular, for a specific T value of about 750 K we observe a rather marked change in the slope and in its sign: a slow increase with temperature at low T and a fast decrease with T as the temperature goes above 1000 K. A possible microscopic explanation for such a behavior could be had by observing again the resonant effects in the total cross sections of Fig. 3. The presence of a large amount of shape resonances (see the upper part of Fig. 3) in the 10^{-3}/0.6-eV energy range counteracts the cross-section decrease with increasing collision energy. In fact, cross sections for the $\Lambda=1$ process, in which the shape resonances are almost absent, turn out to decrease

faster in the 10^{-3}/1-eV energy region than the ones for the $\Lambda=0$ process. At higher collision energies, where resonances are essentially wiped out and not present, cross sections start again to fall off with increasing collision energy, as shown by the upper range of computed total cross sections between 1 and 10 eV of energy. Hence the corresponding high T rates decrease with the temperature increase at roughly similar rates for both processes. In other words, the different nature of the PEC for the $\Lambda=0$ case indicates that in this instance the larger contribution of the resonant enhancements effectively delays to higher T values the decreasing behavior of the recombination rates that is seen instead, even at very low T in the case of the Π-Σ process. This qualitative explanation is well supported by the temperature value at which rate coefficients for the $\Lambda=0$ process show a maximum: 750 K is equivalent to $\sim$65 meV, i.e., a collision energy value that is well inside the region populated by shape resonances, as shown by the partial cross sections of Fig. 2.

IV. CONCLUSIONS

In this paper we have carried out full quantum-mechanical calculations for direct radiative association of the LiH molecule starting from lithium atoms that are electronically excited. Rate coefficients for such a process can be used to estimate LiH abundance in our galaxy, once the fraction of electronically excited lithium in the interstellar medium can be estimated.

As was expected, the process studied turns out to be much more efficient than the one involving atoms in their ground state: rate coefficients are found to be at least five orders of magnitude greater than the ones for the $X\ ^1\Sigma^+ \rightarrow X\ ^1\Sigma^+$ process [4,7], a very interesting result for its astrophysical implications.

We have also studied the influence of the involved potential-energy curve and transition moment features on the final results. Molecular formation turns out to be most probable in excited vibrational states, and the $B\ ^1\Pi \rightarrow X\ ^1\Sigma^+$ process is the more efficient. Shape resonances have a great influence on the final behavior of rate coefficients, especially in the low T regions of the thermal bath of the process.

In general, one can say here that the use of a fully quantum-mechanical treatment of such microscopic processes, i.e., the use of realistic PEC's of accurate transition moments and the fully *ab initio* evaluation of the various channel wave functions (bound and continuum) allows one to generate from first principles, and totally in an *ab initio* fashion, the final quantities that need to be employed to produce a more global modeling of the complex kinetics for the lithium chemistry under different environments.

ACKNOWLEDGMENTS

The financial support of the Italian National Research Council (CNR) and of the Italian Ministry for University and Research (MURST) is gratefully acknowledged. We thank Dr. H. Berriche for having made his results available to us, and Professor F. Melchiorri and Professor A. Dalgarno for making us aware of the problems of lithium chemistry. P.G.G. also thanks Dr. M. Capone for fruitful discussions and suggestions.

[1] P. De Bernardis *et al.*, Astron. Astrophys. **269**, 1 (1993).
[2] R. Maoli, F. Melchiorri, and D. Tosti, Astrophys. J. **425**, 372 (1994).
[3] R. Maoli *et al.*, Astrophys. J. **457**, 1 (1996).
[4] A. Dalgarno, K. Kirby, and P. C. Stancil, Astrophys. J. (to be published).
[5] P. C. Stancil, S. Lepp, and A. Dalgarno, Astrophys. J. (to be published).
[6] F. A. Gianturco, P. Gori Giorgi, H. Berriche, and F. X. Gadea, Astron. Astrophys. Suppl. **117**, 377 (1996).
[7] F. A. Gianturco and P. Gori Giorgi (unpublished).
[8] P. J. E. Peebles, *Principles of Physical Cosmology* (Princeton University Press, Princeton, NJ, 1993).
[9] T. Maiani, F. Melchiorri, and L. Popa (unpublished).
[10] J. F. Babb and A. Dalgarno, Phys. Rev. A **51**, 3021 (1995).
[11] B. Zygelman and A. Dalgarno, Astrophys. J. **365**, 239 (1990).
[12] G. Herzberg, *Spectra of Diatomic Molecules* (Van Nostrand, New York, 1950).
[13] A. Boutalib and F. X. Gadea, J. Chem. Phys. **97**, 1144 (1992).
[14] M. Foucrault *et al.*, J. Chem. Phys. **96**, 1257 (1992).
[15] H. Berriche, thèse d'état, Université Paul Sabatier, Toulouse, France, 1995 (unpublished).
[16] H. Partridge and S. R. Langhoff, J. Chem. Phys. **74**, 2361 (1981).
[17] K. Smith, *The Calculation of Atomic Collision Processes* (Wiley-Interscience, New York, 1971).
[18] R. J. Le Roy and R. B. Bernstein, J. Chem. Phys. **54**, 5114 (1971).
[19] R. J. Le Roy and W. K. Liu, J. Chem. Phys. **69**, 3622 (1978).